



HAL
open science

Regionalized cell proliferation in the symbiont-bearing gill of the hydrothermal vent mussel *Bathymodiolus azoricus*

Bérénice Piquet, François Lallier, Coralie André, Bruce Shillito, Ann Andersen, Sébastien Duperron

► To cite this version:

Bérénice Piquet, François Lallier, Coralie André, Bruce Shillito, Ann Andersen, et al.. Regionalized cell proliferation in the symbiont-bearing gill of the hydrothermal vent mussel *Bathymodiolus azoricus*. *Symbiosis*, 2020, 82, pp.225-233. <10.1007/s13199-020-00720-w>. <hal-03020135>

HAL Id: hal-03020135

<https://hal.sorbonne-universite.fr/hal-03020135v1>

Submitted on 23 Nov 2020

HAL is a multi-disciplinary open access archive for the deposit and dissemination of scientific research documents, whether they are published or not. The documents may come from teaching and research institutions in France or abroad, or from public or private research centers.

L'archive ouverte pluridisciplinaire HAL, est destinée au dépôt et à la diffusion de documents scientifiques de niveau recherche, publiés ou non, émanant des établissements d'enseignement et de recherche français ou étrangers, des laboratoires publics ou privés.



Distributed under a Creative Commons CC BY 4.0 - Attribution - International License

1 **Regionalized cell proliferation in the symbiont-bearing gill of the hydrothermal vent mussel**

2 ***Bathymodiolus azoricus***

3
4 Bérénice Piquet^{1,2,3}, François H. Lallier¹, Coralie André¹, Bruce Shillito², Ann C. Andersen^{1*}, Sébastien
5 Duperron^{3,4,*}

6
7 **1** Sorbonne Université CNRS, Lab. Adaptation et Diversité en Milieu Marin, AD2M, Adaptation et
8 Biologie des Invertébrés marins en Conditions Extrêmes (UMR 7144), ABICE, DYDIV, Station
9 Biologique de Roscoff, place Georges Teissier, Roscoff, France.

10 **2** Laboratoire de Biologie des Organismes et Ecosystèmes Aquatiques (BOREA), MNHN, CNRS-2030,
11 IRD-207, Sorbonne Université, UCN, UA, Team: Adaptation aux Milieux Extrêmes (AMEX), 7 Quai
12 Saint-Bernard, Paris, France

13 **3** Muséum National d'Histoire Naturelle, CNRS, Lab. Mécanismes de Communication et Adaptation
14 des Micro-organismes (UMR 7245), Team: Cyanobactéries, Cyanotoxines et Environnement, CCE,
15 PTME 12 rue Buffon, Paris, France

16 **4** Institut Universitaire de France, Paris, France

17 * Corresponding authors: sebastien.duperron@mnhn.fr and andersen@sb-roscoff.fr

18 S. Duperron ORCID: <https://orcid.org/0000-0002-6422-6821>

19
20
21 **Keywords:** *Bathymodiolus*, EdU, Phosphohistone H3, hydrothermal vents, cell division, chemotrophic
22 symbiosis

23
24 **Acknowledgements**

25 We thank the captain, crew and scientific fellows on board the Research Vessel “*Pourquoi pas?*” and the
26 ROV “*Victor 6000*” (Ifremer) for their invaluable contributions to this work. We thank the RAS Roscoff
27 Aquarium, the Merimage microscopy platform (Roscoff, France), and the fluorescence microscopy
28 facility at Institut de Biologie Paris-Seine. We thank Thermofisher Life Technologies SAS, 91941
29 Courtaboeuf-cedex (Villebon-sur-Yvette), France, for providing an initial Click-IT EdU test that proved
30 to be successful.

31 **Abstract**

32 Deep-sea mussels *Bathymodiolus* spp. harbor high densities of chemosynthetic bacterial
33 symbionts located within their gill epithelial cells. Compared to non-symbiotic coastal mussel relatives
34 of similar size, *Bathymodiolus* gills are considerably larger, a feature often considered an adaptation to
35 symbiosis because it is related to the presence of intracellular bacteria in epithelial cells located in the
36 lateral zone. In order to document the mechanisms underlying these sizes differences, this study
37 compares gill cell proliferation patterns in *Bathymodiolus azoricus* and *Mytilus edulis* using microscopy-
38 based approaches. We used incubation experiments with a synthetic nucleotide (5-ethynyl 2'-
39 deoxyuridine, EdU), detectable throughout novel cell divisions, and phosphohistone H3
40 immunolabeling, a marker of mitosis. The results revealed proliferation areas in the ciliated zone and in
41 the bacteria-loaded bacteriocytes located close to the frontal zone of gill filaments, swept by the
42 incurrent sea-waterflow, and also in the dorsal region of gills in *B. azoricus*. Cell proliferation seems far
43 less intensive in *M. edulis*. This study overall suggests high cell turnover and fast tissue dynamics in
44 symbiont-bearing mussels.

45

46 **Introduction**

47

48 Tissues and organs that have evolved to host intracellular microorganisms are common in
49 various animal taxa, including the endoderm of cnidarians, insect bacteriomes, and the trophosome of
50 deep-sea tubeworms (Russel and Ruelas Castillo, 2020). In a multicellular organism, the number of
51 microbes within each host cell, as well as the size of symbiont-hosting tissues must be regulated in a
52 way that does not compromise proper host development and maintenance. However, to understand the
53 adaptations that underpin an organ's ability to host symbionts, a comparative approach is mandatory, in
54 which patterns can be compared in the same organ between symbiont-containing and non-symbiotic
55 related species.

56 Large Bathymodiolinae mussels from deep-sea hydrothermal vents and cold seeps offer an
57 interesting opportunity to study how an organ may evolve to become symbiotic. As members of the
58 family Mytilidae, symbiotic Bathymodiolinae can be compared with coastal Mytilidae that have no
59 symbionts. The gills of adult Bathymodiolinae indeed harbor bacterial symbionts in high densities, in
60 the range of 10^{12} per individual, within specialized gill epithelial cells named bacteriocytes. Their gills
61 are enlarged, representing an exchange surface about 20-fold larger than that of a similar-sized *Mytilus*
62 *edulis* (Duperron et al. 2016). Finally, *Bathymodiolus* species can be kept in aquaria at atmospheric
63 pressure for extended periods of time, up to several months, facilitating experimental work (Kadar et al.
64 2005).

65 Most *Bathymodiolus* species (e.g. *B. thermophilus*) host sulfur-oxidizing autotrophic bacteria
66 that use reduced compounds present in environmental fluids as energy sources, and fix carbon through
67 the Calvin-Benson cycle, a process called chemosynthesis. Other *Bathymodiolus* (e.g. *B. platifrons*)

68 have methane-oxidizing bacteria that use methane as both carbon and energy source. Finally, a few
69 species (e.g. *B. azoricus*, *B. puteoserpentis* and *B. cf. boomerang*) harbor both symbiont types
70 simultaneously inside the same gill epithelial cells (Duperron 2010; Assié et al. 2016; Ponnudurai et al.
71 2017). Symbionts are acquired from the environment at the post-larval stage, and gill epithelial cells
72 remain competent to acquire bacteria throughout host's life, resulting in coexistence of multiple related
73 symbiont strains (Wentrup et al. 2013; Ansorge et al. 2019). This symbiosis is highly flexible i.e.
74 symbiont's nature and abundances can be modulated by environmental and metabolic host factors.
75 Indeed, symbionts rapidly disappear when their substrates start to run out, and the relative abundances
76 of sulfur- versus methane-oxidizers can vary in response to respective substrate availability (Halary et
77 al. 2008; Szafranski et al. 2015). Moreover, bacterial turn-over inside cells results from bacterial
78 divisions on the one hand, and digestion in phagolysosome-like structures by which hosts get their food,
79 on the other hand (Fiala-Medioni et al. 1994; Dubilier et al. 1998). However, the mechanisms that allow
80 for gill hypertrophy in *Bathymodiolus* are poorly understood. A recent study investigated the role of
81 apoptosis in the regulation of symbiosis and gill tissue in two *Bathymodiolus* species, one from the Mid-
82 Atlantic ridge hydrothermal vents and one from the Regab cold seep site (Piquet et al. 2019). In both
83 *Bathymodiolus* species, apoptotic levels were highest in the ciliated frontal zone of the gill filaments,
84 (which all together build the side of the gill lamella that is swept by the incurrent seawater flow), and in
85 the circulating hemocytes. It was hypothesized that apoptosis was a consequence of high activity levels
86 of ciliated cells and associated oxidative stress, involving immunity responses from hemocytes of the
87 mussel. The apoptotic rate was comparatively lower in bacteriocytes, in which apoptosis most often
88 occurred in the abfrontal region of the gill filament, opposite to the incurrent seawater flow, where
89 symbionts were least abundant, suggesting ongoing elimination of these bacteriocytes through
90 apoptosis.

91 To maintain the gills hypertrophy, high apoptotic rates must be compensated by high
92 proliferation rates. In this study, we investigated gill cells proliferation patterns in *Bathymodiolus*
93 *azoricus* mussels using microscopic labeling approaches. For this, mussels were incubated
94 experimentally in the presence of a synthetic nucleotide, EdU (5-ethynyl 2'-deoxyuridine), that replaced
95 thymidine in newly synthesized DNA and was revealed by fluorescence microscopy in cell nuclei. As a
96 complementary approach, phosphohistone H3, a marker of mitosis commonly used in cell proliferation
97 studies, was labeled with a fluorescent antibody. The same experiments were performed in parallel on
98 the non-symbiotic mussel *Mytilus edulis* for comparison. To our knowledge, this study offers the first
99 attempt to document cell proliferation patterns in deep-sea mussel gills and their relationship with
100 symbiosis.

101

102 **Materials and methods**

103

104 ***Specimen sampling, EdU incubations and vizualisation***

105 *Bathymodiolus azoricus* specimens were collected with the ROV Victor 6000 during the
106 MOMARSAT / BioBaz 2017 cruise (Sarradin and Cannat 2017) on the Lucky Strike site, at the Eiffel
107 Tower edifice (37°17.333N; 32°16.541W, 1690m depth, mean shell length: 71.3 ± 16.9 mm).
108 Immediately upon recovery, 4 mussels were cut open in the cold room (4°C) and the gills were dissected
109 without damaging the tissue. Labeling was performed using EdU as an alternative to BrdU (5-bromo-
110 2'-deoxyuridine). Attempts with BrdU according to classical protocols (Gratzner 1982; Zaldibar et al.
111 2004; Gómez-Mendikute et al. 2005; Elisabeth et al. 2012) were also performed on both entire animals
112 and on excised gills, but resulted in low-quality labeling due to tissue damage during the mandatory step
113 of hydrochloric acid denaturation of the tissue (not shown). Moreover, incubations of excised gills of *B.*
114 *azoricus* on board ensured a direct and time-controlled exposure of the tissues with the marker, whereas
115 incubation of live bivalves with either BrdU or EdU requires greater concentrations and may result in
116 hermetic closure of their shells, which prevents any labeling in the gills.

117 One gill of each specimen was placed at ambient pressure in a Petri dish containing 0.22µm-
118 filtered surface sea water (SFSW) and incubated with Click-itTM EdU (5-ethynyl 2'-deoxyuridine,
119 Invitrogen), at 4°C. Three EdU concentrations were tested : 3, 30 and 100 mg.L⁻¹, during 2 hours
120 incubation experiments (due to onboard constraints), and one gill was incubated for 48 hours (as a very
121 long maximum time) in 3 mg.L⁻¹ EdU. Similar incubations in the presence of EdU, with 5 hours
122 incubation time, were performed on dissected gills of *Mytilus edulis* collected in Bloscon harbor at
123 Roscoff (48°42.975N, 3°57.835W, mean shell length: 47.3 ± 2.0 mm), and maintained for one month in
124 Roscoff aquarium service (RAS, 8 °C, filtered natural seawater, fed daily with *Isochrysis* microalgae).
125 It must be noted that *Mytilus* mussels remained alive and active throughout this period.

126 Gills were fixed individually after each experiment using 3.7% formaldehyde in SFSW, rinsed
127 in SFSW, dehydrated in increasing ethanol series, then embedded in Steedman resin as described in
128 Duperron (2015). Sections (8 µm-thick) were cut on a microtome (Thermo, UK) and placed on
129 SuperFrost Plus slides (VWR, France). Resin was then removed using ethanol. Sections were rehydrated
130 (1X PBS) and permeabilized (0.1% Triton X-100 and 5% BSA in 1X PBS, RT, 30 min). Then, 100 µl
131 of the solution included in the “Click it” EdU Kit (Invitrogen, USA) were placed on each slide, for 30
132 min in a dark room. This solution contains azide coupled to the FITC-fluorochrome, and CuSO₄ which
133 catalyzes the reaction. Slides were then rinsed and mounted with Hoechst (Invitrogen, USA) and
134 Vectashield (Clinisciences, Nanterre, France). Slides were observed under a confocal SP5 microscope
135 (Leica, Germany) using filters for DAPI/Hoechst (excitation wavelength: 351 nm; emission at 415-
136 492nm) and EdU (excitation wavelength: 488 nm; emission at 501-602 nm).

137

138 ***Specimen sampling and phosphohistone H3 (PH3) labeling***

139 PH3 labeling was performed on *Bathymodiolus azoricus* specimens collected during the BioBaz
140 2013 cruise (Lallier 2013) on two sites of the Mid-Atlantic ridge, namely Menez Gwen (MG2 marker;
141 37°50.669N; 31°31.156W, 830m depth, 3 specimens, mean shell length: 62.8 ± 26.9 mm) and Rainbow

142 (France 5 marker; 37°17.349N; 32°16.536W, 2270m depth, 4 specimens, mean shell length not
143 recorded). Specimens were sampled using the pressure-maintaining device PERISCOP that retains
144 deep-sea pressure and temperature throughout the recovery process (Shillito et al 2008). Labeling was
145 also performed on 4 specimens of *M. edulis* from the same sample as above. Gills were fixed, embedded,
146 sectioned and sections were rehydrated as above. Slides were permeabilized in 2% BSA; 0.3% Triton
147 X-100 in PBS (2 h, RT). The primary anti-PH3 antibody (polyclonal Ser 10, Merck, Germany) was
148 deposited ($5 \mu\text{g}.\text{ml}^{-1}$; 2 hours RT or overnight at 4°C). Negative controls were performed by omitting
149 the primary antibody. Slides were then rinsed and incubated with the secondary antibody (goat anti-
150 rabbit, Invitrogen, USA) coupled to the fluorochrome Alexa Fluor 488 ($5\mu\text{g}.\text{ml}^{-1}$, 1h, dark humid room).
151 Slides were then rinsed and mounted in DAPI-containing Slow Fade (Life Technologies). They were
152 observed under a confocal SP5 microscope (Leica, Germany) using filters for DAPI/Hoechst (excitation
153 wavelength: 351 nm; emission at 415-492nm) and Alexa 488 (excitation wavelength: 488 nm; emission
154 at 505-655 nm). Images were processed using Image J (Abràmoff et al. 2004).

155

156 **Results**

157

158 ***EdU labeling reveals differences of proliferation patterns between symbiotic Bathymodiolus and*** 159 ***non-symbiotic Mytilus mussels***

160 Non-ambiguous and sharp labeling was found in gills of *B. azoricus* from Lucky Strike
161 incubated at $3 \text{ mg}.\text{L}^{-1}$ EdU for 48 hours (figure 1), and at the three EdU concentrations for 2 hours (figure
162 2). As expected for a DNA-based labeling method, the EdU signals were located in cell nuclei,
163 superimposed with Hoechst labeling. The cell proliferation pattern shown in Fig 1 and 2 was observed
164 in all examined filaments. Ciliated cells located at the frontal end of the gill filaments were frequently
165 labeled (figures 1 and 2). The frontal ends together build the side of the gill lamellae swept by the
166 incurrent water flow (figure 1A). In the bacteriocytes zone, dividing cells were more frequent in the
167 bacteriocytes located closest to this frontal zone, (figures 1 and 2). Very few dividing cells were visible
168 in the abfrontal zone (abfrontal ends assembled together build the inner side of each V-shaped gill
169 lamellae, closer to the excurrent flow, see figure 1A). Random and sparse EdU labeling was observed
170 in the lateral zone (figure 1B-E), i.e in the thickness of the gill lamellae, where filaments are aligned
171 side by side, joined by inter-filament ciliary junctions (figure 1A). In the dorsal zone of the gill, where
172 the gill lamellae attach to the visceral mass, cells are not yet fully differentiated. Thus, in the dorsal
173 region ciliated cells and bacteriocytes cannot be identified, however many nuclei were randomly labeled,
174 but not specifically facing the frontal zone (figure 1 B).

175 In *Mytilus edulis*, few, yet unambiguous labeling was visible at all three EdU concentrations
176 tested. Dividing cells were scattered throughout the gill filaments, mainly in the lateral zones, without
177 any apparent regionalization or clear pattern (figure 3). Interestingly, contrary to *B. azoricus*, the frontal
178 zones were not labeled in *M. edulis*.

179

180 ***Phosphohistone H3 labeling confirms the occurrence of cell divisions***

181 A few gill cells of *B. azoricus* from both Menez Gwen site and the deeper Rainbow site were
182 successfully labeled with the PH3-specific antibody. Few labeled nuclei (yet unambiguously labeled)
183 were observed in any given filament section (figure 4A-E). Signals were sharp and consisted of ring-
184 like labels around a nucleus (figure 4B-D), or crescent-like labeling on the distal halves of nuclei of two
185 sister-cells (figure 4E). These were detected in all 7 investigated specimens, from both vent sites. The
186 best staining results were obtained after 2 hours incubation with the primary antibody. In gill filaments,
187 PH3 labeling mostly occurred on nuclei of non-ciliated gill epithelial cells. Qualitatively, dividing cells
188 appeared more abundant on sections from the dorsal region of gills, in the zone of attachment to the
189 visceral mass, where cell types cannot be distinguished, and where DAPI staining reveals a high density
190 of nuclei (figure 4A). No PH3 labeling was present in a total of 10 slides (each comprising several
191 individual filaments) from the four individuals of *M. edulis* (not shown).

192

193 **Discussion**

194

195 ***Bathymodiolus azoricus* gills display regionalized cell proliferation patterns**

196 Clear evidence of cell division on excised gills of both *B. azoricus* and *M. edulis* mussels was
197 observed, even at the lowest tested EdU concentration (3mg.L⁻¹). Because EdU labeling relies on direct
198 fluorescence of the synthetic nucleotide rather than on antibody revelation, the protocol is faster with
199 less permeabilization steps, and thus ensures a better conservation of the tissue structure. To our
200 knowledge, this study is the first application of the EdU protocol on bivalve mollusks and demonstrates
201 its relevance for the study of cell proliferation patterns in this taxon.

202 Both EdU and PH3 labeling support the evidence of cell proliferation in the dorsal zone of *B.*
203 *azoricus* gill filaments, where the filaments attach to the mussel's visceral mass. This corroborates
204 previous results by Wentrup et al. (2014) showing abundant proliferating cell nuclear antigen (PCNA)
205 signals in the nuclei of host cells in both juvenile and adult *B. puteoserpentis* at dorsal ends of gills. This
206 dorsal region initially corresponds to a symbiont-free area (Wentrup et al., 2014). According to our
207 results, a continuous dorsal growth seems to occur in *B. azoricus*. The ventral zone of the gill filaments
208 is also known to be a growth zone in mussels (Wentrup et al., 2014). However, in the ventral zone our
209 results are not conclusive as the PH3 staining did not exactly co-localize with nuclei. However, towards
210 the ventral part of the gill filaments, we saw EdU labelled cell divisions in the frontal zones (see Fig.1E).
211 The frontal zones are also ciliated cells that are devoid of symbionts. Thus, proliferation of the ciliated
212 cells appears particularly abundant in two symbiont-free zones of the *B. azoricus* gill, namely the dorsal
213 and the frontal zones. In the bacteriocytes of *B. azoricus*, which are not ciliated, cell divisions mainly
214 occurred in bacteriocytes close to the frontal ciliated zone. These bacteriocytes are heavily loaded with
215 bacteria (Pernthaler et al. 2008; Wentrup et al. 2014; Piquet et al. 2019). Bacteriocytes located in the

216 abfrontal zone, which generally contain fewer symbionts, were almost never undergoing cell division.
217 Despite only qualitative, these observations suggest a regionalized pattern of cell proliferation in *B.*
218 *azoricus*.

219 Experiments on excised gills of symbiont-free *Mytilus edulis* yielded far less abundant EdU
220 labeling with a random distribution in the gill filaments, suggesting that EdU labeling did work, and that
221 proliferation is possibly less regionalized in this species. It must be noted that bacteriocytes found in
222 *Bathymodiolus* are never ciliated and do not exist in *Mytilus*, while on the contrary, in *Mytilus* all gill
223 cells are ciliated throughout the gill lamellae. Interestingly though, frontal ciliated cells exist in both
224 species, and were often labeled in *Bathymodiolus*, while they were rarely labeled in *Mytilus*. However,
225 the reasons for this striking difference could also be biological, for example due to the metabolic state
226 of the *M. edulis* individuals kept in the aquaria. Moreover, experiments with BrdU on *M. edulis* digestive
227 gland have shown that cell proliferation is far more active in summer than in autumn and winter, and
228 that in intertidal mussels, unlike in subtidal specimens, cell divisions are modulated by a photoperiod
229 with variations following a circa-tidal pattern (Zaldibar et al. 2004, 2008), which might be valid in other
230 tissues as well. Although our coastal mussels were subtidal, an environmentally triggered clock cannot
231 be ruled out, resulting in *M. edulis* not being in an active phase of cell divisions during our experiment.
232 Thus, the differences in the cell divisions evidenced here between the two mussel-species must be taken
233 with caution.

234 Positive labeling using the PH3-specific antibody are in line with previous positive results
235 observed in the symbiotic lucinid clam *Codakia orbiculata* (Elisabeth et al. 2012) and confirm that the
236 antibody is suitable for the monitoring of bivalve cell mitosis, despite it initially was used in mammalian
237 studies (Henzel et al. 1997; Hans and Dimitrov 2001; Li et al. 2005). Abundance and patterns of PH3
238 labeling confirm that cells are undergoing mitosis in *B. azoricus* gills, possibly more in the dorsal region
239 of the gills. *Mytilus edulis* gills did not yield labeling, suggesting lower levels of mitosis, but one cannot
240 rule out the alternative hypothesis that the antibody did not work in this species. The existence of
241 physiological differences between mussels from Lucky Strike (used for EdU labeling) and mussels from
242 Menez Gwen and Rainbow (used for PH3 labeling) might explain observed differences in signal
243 abundance between EdU and PH3 in *B. azoricus*. However, low abundance of PH3 compared to EdU
244 labeling is not surprising. Indeed, EdU is replacing Thymidine in DNA during the S-phase, and remains
245 detectable throughout novel cell divisions (i.e. S-, G2- and M-phases). Thus, EdU is still visible in
246 daughter cells long after they have finished dividing. PH3 on the other hand participates to chromatin
247 condensation, and is only detectable during mitosis (i.e. M-phase), particularly during metaphase
248 (Henzel et al. 1997). Once mitosis is over, PH3 labeling is not visible anymore, contrary to EdU.

249 Overall, EdU and PH3 labeling gave qualitatively congruent results. Based on EdU, cell
250 proliferation in *B. azoricus* seems to be higher in the ciliated cells of the frontal zone and possibly in the
251 bacteriocytes located closest to these ciliated cells. Both EdU and PH3 labeling support that a cell
252 proliferation zone exists in the dorsal region of the gill, supporting that the dorso-ventral growth zone

253 of the gill could be due to cell divisions occurring in this region. This dorsal growth zone confirms some
254 of the results obtained by Wentrup et al. (2014) showing abundant proliferating cell nuclear antigen
255 (PCNA) signals in the nuclei of host cells in both juvenile and adult *B. puteoserpentis* at dorsal ends of
256 gills. The dorsal attachment point is also the ontogenic growth zone in *M. edulis* (Cannuel et al. 2009).
257 Yet, patterns in *M. edulis* gills suggest a far less dynamic tissue, with lower abundance and more even
258 distribution of both EdU and PH3 labeling.

259

260 ***A hypothetical model for the overall dynamics of the symbiont-containing gill of B. azoricus***

261 A recent study has investigated the patterns of apoptosis in the gills of two *Bathymodiolus*
262 species including *B. azoricus* from the same sites considered here (Piquet et al. 2019). Apoptosis was
263 regionalized, and levels were higher than in *Mytilus edulis*. The highest apoptosis rates were measured
264 in the frontal ciliated cells. Higher metabolic activity (and thus oxidative stress of these cells), associated
265 with the larger size of gills, and/or toxic effects associated with the sulfide-enriched fluid from the
266 incurrent seawater flow influenced by hydrothermal fluid, were hypothesized to result in higher
267 apoptotic rates compared to non-symbiotic mytilids. Our study indicates that the frontal ciliated zone is
268 also an area of cell proliferation, suggesting a rapid cell turn-over in this region. Our hypothesis is a
269 necessarily intense and frequent renewal of the frontal ciliated cells that are in the first line, when swept
270 by the incurrent flow containing possible xenobiotics arising from the hydrothermal vents, although the
271 cause for such a phenomenon remains to be determined. By combining the observations on apoptosis
272 and proliferation, we propose a model for the dynamics of the symbiont-containing gill of *B. azoricus*
273 (figure 5).

274 In the bacteriocytes zone, apoptosis was more frequent in bacteriocytes located in the abfrontal
275 zone, opposite to the frontal zone, an area where bacterial symbionts are less abundant. Our study shows
276 that proliferation on the other hand occurs in bacteriocytes closest to the frontal zone, where symbionts
277 are the most abundant. We hypothesize that increased cell divisions of these bacteriocytes contribute to
278 increase the total symbiont load. Indeed, upon bacteriocyte division, each daughter cell may inherit host
279 bacterial symbionts, from which its symbiotic population may further grow (by bacterial symbiont
280 division). This could explain some patterns described years ago from cold seep *Bathymodiolus heckeriae*,
281 in which two different sulfur-oxidizing symbionts seemed to colonize distinct patches of bacteriocytes
282 within a given filament (figure 2E-F in Duperron et al. 2007). Under this hypothesis, each individual
283 patch could correspond to daughter cells of distinct initial bacteriocytes that contained one or the other
284 type of symbiont. Alternatively, but not exclusively, daughter cells may be colonized by bacteria
285 released from other bacteriocytes in neighbor gill filaments, as observed in the posterior budding zone
286 of gills from *B. azoricus* and *B. puteoserpentis* (Wentrup et al. 2014). The fact that new host cells are
287 produced where symbionts are the most abundant might be an efficient mechanism to maximize the
288 bacterial load in the gill, producing more available space for bacterial growth (figure 5).

289 The model (Fig. 5) shows a cross section of a gill filament and highlights the zones where cell-
290 division and apoptosis were observed in our experiments. In summary, the external side of the gill
291 lamellae is constituted by ciliated cells that alternatively undergo apoptosis and cell division, attesting
292 of an intense cellular renewal in this frontal zone, swept by the incurrent water flow. In the thickness of
293 the gill filaments (i.e. the lateral zone), the bacteriocytes closest to the frontal zone were often in cell
294 division, putatively enabling to enhance their load of bacterial symbionts. On the contrary, bacteriocytes
295 close to the abfrontal zone, swept by the excurrent flow, were often in apoptosis. Whether cell divisions
296 and apoptosis are two successively alternating processes within each zone, or whether there is a
297 migration of replicating cells, from the frontal to the abfrontal zone cannot be discriminated from our
298 observations. Indeed, both cell renewal occurring by division of existing cells, and division of
299 undifferentiated putative "stem-cells" migrating afterwards are documented in the symbiotic *Codakia*
300 lucinid by Elisabeth et al., (2012). Ultrastructural studies in *B. azoricus* gills are required to further shed
301 light into these putative cellular processes.

302

303 To better understand patterns of gill development, future work should focus on the dorsal (for
304 dorso-ventral growth) and posterior budding (for antero-posterior growth) zones of the gill in specimens
305 at various life stages using similar labeling techniques. Finally, the molecular mechanisms that underlie
306 gill tissue dynamics, and the influence of bacterial symbionts on hosts processes, remain to be
307 investigated. Spatial metabolomic at the cellular level seems a promising tool to entangle host-microbe
308 interactions (Geier et al., 2020). These host and symbiont mechanisms may have major roles in the
309 reported adjustments and overall plasticity reported in the association between mussels and
310 chemosynthetic bacteria, which is considered key to their ecological success.

311

312 **References**

313 Abràmoff MD, Magalhães PJ, Ram SJ (2004) Image processing with ImageJ. *Biophotonics Int* 11:36–
314 42. <https://doi.org/10.1016/j.tcb.2004.03.002>

315 Ansoerge R, Romano S, Sayavedra L, et al (2019) Functional diversity enables multiple symbiont
316 strains to coexist in deep-sea mussels. *Nat Microbiol* 4:2487–2497. <https://doi.org/10.1038/s41564-019-0572-9>

318 Assié A, Borowski C, van der Heijden K, et al (2016) A specific and widespread association between
319 deep-sea *Bathymodiolus* mussels and a novel family of Epsilonproteobacteria: Epsilonproteobacterial
320 epibionts of *Bathymodiolus*. *Environ Microbiol Rep* 8:805–813. <https://doi.org/10.1111/1758-2229.12442>

322 Cannuel R, Beninger PG, McCombie H, Boudry P (2009) Gill development and its functional and
323 evolutionary implications in the blue mussel *Mytilus edulis* (Bivalvia: Mytilidae). *Biol Bull* 217:173–
324 188. <https://doi.org/10.1086/BBLv217n2p173>

325 Dubilier N, Windoffer R, Giere O (1998) Ultrastructure and stable carbon isotope composition of the
326 hydrothermal vent mussels *Bathymodiolus brevior* and *B. sp. affinis brevior* from the North Fiji Basin,
327 western Pacific. *Mar Ecol Prog Ser* 165:187–193. <https://doi.org/10.3354/meps165187>

328 Duperron S (2010) The diversity of deep-sea mussels and their bacterial symbioses. In: Kiel S (ed)
329 *The Vent and Seep Biota*. Springer Netherlands, Dordrecht, pp 137–167

330 Duperron S (2015) Characterization of bacterial symbionts in deep-sea fauna: protocols for sample
331 conditioning, fluorescence in situ hybridization, and image analysis. In: McGenity TJ, Timmis KN,
332 Nogales B, editors. *Hydrocarbon and Lipid Microbiology Protocols*. Berlin, Heidelberg: Springer
333 Berlin Heidelberg. pp. 343–362. https://doi.org/10.1007/8623_2015_73

334 Duperron S, Quiles A, Szafranski KM, et al (2016) Gill surface areas and symbionts abundances in the
335 hydrothermal vent mussel *Bathymodiolus puteoserpentis* maintained in pressure vessels. *Front. Mar.*
336 *Sci.* 16. <https://doi.org/10.3389/fmars.2016.00016>

337 Duperron S, Sibuet M, MacGregor BJ, et al (2007) Diversity, relative abundance and metabolic
338 potential of bacterial endosymbionts in three *Bathymodiolus* mussel species from cold seeps in the
339 Gulf of Mexico. *Environ Microbiol* 9:1423–1438. <https://doi.org/10.1111/j.1462-2920.2007.01259.x>

340 Elisabeth NH, Gustave SDD, Gros O (2012) Cell proliferation and apoptosis in gill filaments of the
341 lucinid *Codakia orbiculata* (Montagu, 1808) (Mollusca: Bivalvia) during bacterial decolonization and
342 recolonization. *Microsc Res Tech* 75:1136–1146. <https://doi.org/10.1002/jemt.22041>

343 Fiala-Medioni A, Michalski J, Jollès J, et al (1994) Lysosomal and lysozyme activities in the gill of
344 bivalves from deep hydrothermal vents. *CR Acad Sci Sci VieLife Sci* 317:239–244

345 Geier B, Sogin EM, Michellod D, Janda M, Kompauer M, Spengler B, Dubilier N & Liebecke M.
346 (2020). Spatial metabolomics of in situ host–microbe interactions at the micrometre scale. *Nature*
347 *Microbiology* 5 (3): 498-510

348 Gómez-Mendikute A, Elizondo M, Venier P, Cajaraville MP (2005) Characterization of mussel gill
349 cells *in vivo* and *in vitro*. *Cell Tissue Res* 321:131–140. <https://doi.org/10.1007/s00441-005-1093-9>

350 Gratzner HG (1982) Monoclonal antibody to 5-Bromo- and 5-Iododeoxyuridine: A new reagent for
351 detection of DNA replication. *Science* 218:474–475

352 Halary S, Riou V, Gaill F, et al (2008) 3D FISH for the quantification of methane-and sulphur-
353 oxidizing endosymbionts in bacteriocytes of the hydrothermal vent mussel *Bathymodiolus azoricus*.
354 *ISME J* 2:284–292

355 Hans F, Dimitrov S (2001) Histone H3 phosphorylation and cell division. *Oncogene* 20:3021–3027

356 Hendzel MJ, Wei Y, Mancini MA, et al (1997) Mitosis-specific phosphorylation of histone H3
357 initiates primarily within pericentromeric heterochromatin during G2 and spreads in an ordered
358 fashion coincident with mitotic chromosome condensation. *Chromosoma* 106:348–360

359 Kadar E, Bettencourt R, Costa V, et al (2005) Experimentally induced endosymbiont loss and re-
360 acquisition in the hydrothermal vent bivalve *Bathymodiolus azoricus*. *J Exp Mar Bio Ecol* 318:99–
361 110

362 Lallier F (2013) BIOBAZ 2013 cruise, Pourquoi pas ? R/V. <https://doi.org/10.17600/13030030>

363 Li DW, Yang Q, Chen JT, et al (2005) Dynamic distribution of Ser-10 phosphorylated histone H3 in
364 cytoplasm of MCF-7 and CHO cells during mitosis. *Cell Res* 15:120

365 Pernthaler A, Dekas AE, Brown CT, et al (2008) Diverse syntrophic partnerships from deep-sea
366 methane vents revealed by direct cell capture and metagenomics. *Proc Natl Acad Sci* 105:7052–7057

367 Piquet B, Shillito B, Lallier FH, et al (2019) High rates of apoptosis visualized in the symbiont-
368 bearing gills of deep-sea *Bathymodiolus* mussels. *PLOS ONE* 14:e0211499.
369 <https://doi.org/10.1371/journal.pone.0211499>

370 Ponnudurai R, Kleiner M, Sayavedra L, et al (2017) Metabolic and physiological interdependencies in
371 the *Bathymodiolus azoricus* symbiosis. *ISME J.* 11:463-477 <https://doi.org/10.1038/ismej.2016.124>

372 Russell S, Ruelas Castillo J (2020) Trends in Symbiont-Induced Host Cellular Differentiation.
373 Available at preprints.org. <https://doi.org/10.20944/preprints202004.0172.v2>

374 Sarradin P-M, Cannat M (2017) MOMARSAT2017 cruise, Pourquoi pas ? R/V

375 Szafranski KM, Piquet B, Shillito B, et al (2015) Relative abundances of methane- and sulfur-
376 oxidizing symbionts in gills of the deep-sea hydrothermal vent mussel *Bathymodiolus azoricus* under
377 pressure. *Deep Sea Res Part Oceanogr Res Pap* 101:7–13. <https://doi.org/10.1016/j.dsr.2015.03.003>

378 Shillito B, Hamel G, Duchi C, Cottin D, Sarrazin J, Sarradin P-M, et al. Live capture of megafauna
379 from 2300m depth, using a newly designed Pressurized Recovery Device. *Deep Sea Res Part*
380 *Oceanogr Res Pap* 2008; 55:881–9. <https://doi.org/10.1016/j.dsr.2008.03.010>

381 Wentrup C, Wendeberg A, Huang JY, et al (2013) Shift from widespread symbiont infection of host
382 tissues to specific colonization of gills in juvenile deep-sea mussels. *ISME J* 7:1244–1247.
383 <https://doi.org/10.1038/ismej.2013.5>

384 Wentrup C, Wendeberg A, Schimak M, et al (2014) Forever competent: deep-sea bivalves are
385 colonized by their chemosynthetic symbionts throughout their lifetime: Symbiont colonization in gills
386 of deep-sea bivalves. *Environ Microbiol* 16:3699–3713. <https://doi.org/10.1111/1462-2920.12597>

387 Zaldibar B, Cancio I, Marigomez I (2004) Circatidal variation in epithelial cell proliferation in the
388 mussel digestive gland and stomach. *Cell Tissue Res* 318:395–402. [https://doi.org/10.1007/s00441-](https://doi.org/10.1007/s00441-004-0960-0)
389 [004-0960-0](https://doi.org/10.1007/s00441-004-0960-0)

390 Zaldibar B, Cancio I, Marigómez I (2008) Epithelial cell renewal in the digestive gland and stomach
391 of mussels: season, age and tidal regime related variations. *Histol Histopathol* 23:281–290.
392 <https://doi.org/10.14670/HH-23.281>

393

394 **Declarations**

395 **Funding**

396 BP was funded through a joint grant from Région Bretagne and Sorbonne University (project
397 FlexSyBi) and labwork was funded by Institut Universitaire de France project ACSYMB. The
398 pressure-maintaining device PERISCOP was funded by the EC project EXOCET/D (FP6-GOCE-CT-
399 2003-505342). The funders had no role in study design, data collection and analysis, decision to
400 publish, or preparation of the manuscript.

401 **Conflicts of interest/Competing interests** (include appropriate disclosures)

402 The authors have declared that no competing interests exist.

403

404 **Ethics approval**

405 No specific permissions were required for the sampled locations, and the study did not involve
406 endangered or protected species.

407

408 **Consent to participate:** not applicable

409 **Availability of data and material**

410 All relevant data are within the manuscript.

411 **Authors' contributions**

412 SD, ACA and BP designed the study, analyzed the data and wrote the original draft of the manuscript.

413 SD, ACA, BS and FHL obtained the funding

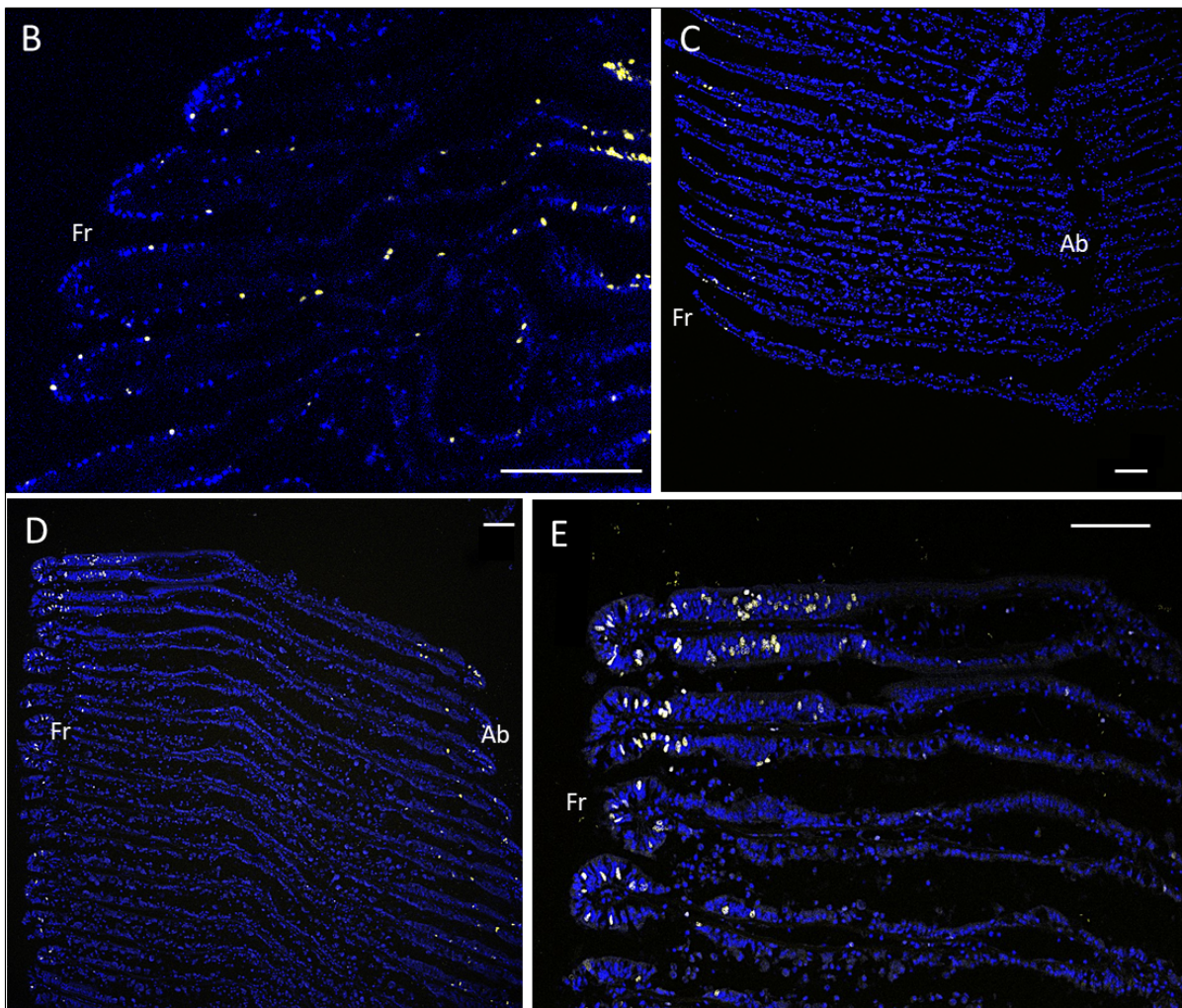
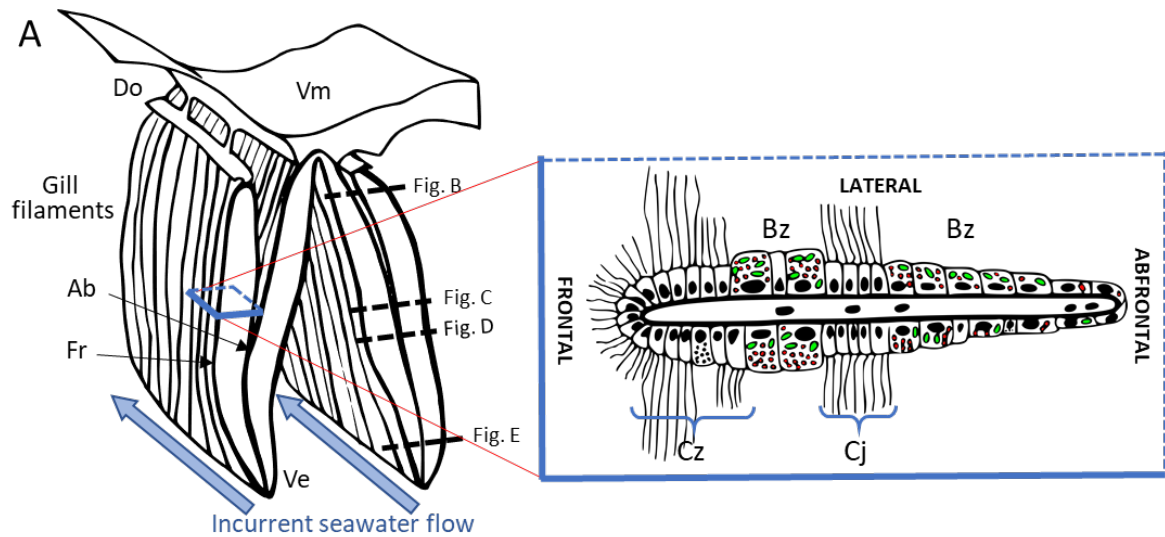
414 BP and CA conducted the labwork

415 FHL and BS were involved in study design, field work during cruises.

416 All authors have read, reviewed, and agreed on the manuscript.

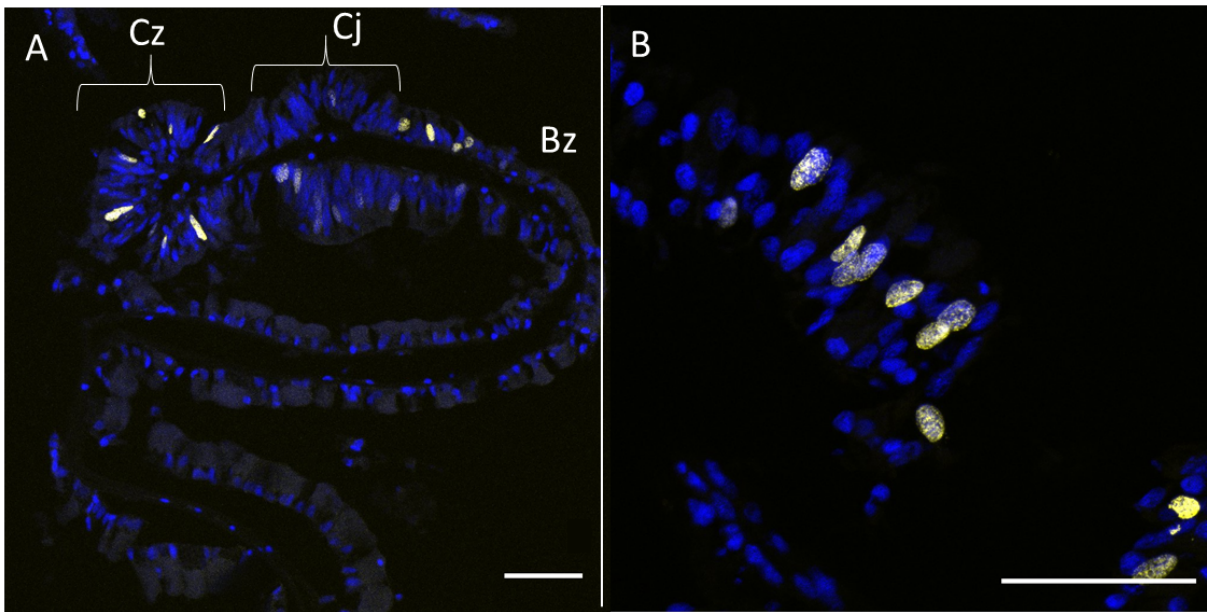
417

418



419
 420 **Figure 1:** Serial gill cross sections of *Bathymodiolus* and associated EdU and Hoechst labeling. **A:** localization
 421 of sections in the dorso-ventrally oriented (Do; Ve) W-shaped gill, attached in its dorsal part to the visceral mass
 422 (Vm), displaying the orientation of individual gill filaments (frontal; Fr and abfrontal Ab; modified from Le Penec
 423 and Hily, 1984); and (right) detail of a gill filament section composed of frontal, lateral and abfrontal zones.
 424 Frontal sides refer to the external sides of the gill lamellae directly facing the seawater current within the mantle
 425 cavity, while the abfrontal sides refer to their inner sides, facing either V-shaped cavity of the gills. Host nuclei

426 are in black, while sulfur- and methane-oxidizing symbionts are in red and green, respectively. The frontal zone
427 consists of ciliated cells (Cz), the lateral includes bacteriocytes zones (Bz) as well as ciliated junctions (Cj), while
428 the abfrontal zone consists of thinner bacteriocytes with very few symbionts. **B-E:** EdU labeling ($3\text{mg}\cdot\text{L}^{-1}$ EdU,
429 48 hours) on some of the 14 obtained serial sections, cut from the dorsal (B) to the more ventral region of the gill
430 (E). Hoechst (blue) labels the nuclei and symbiotic bacteria, and EdU (yellow) labels the nuclei of the cells which
431 have undergone cell division during EdU incubation. Note the comparative abundance of labeled cells and their
432 distribution in the dorsal region (B), compared to the more ventral region (C-E) where most of the EdU-labeled
433 cells are located in the frontal zone of the filaments, while abfrontal zones are mostly devoid of labeling. Very few
434 cells appear labeled in the bacteriocyte zone where bacteriocytes and ciliated junctions also are present. Scale
435 bars: $100\ \mu\text{m}$.
436



438

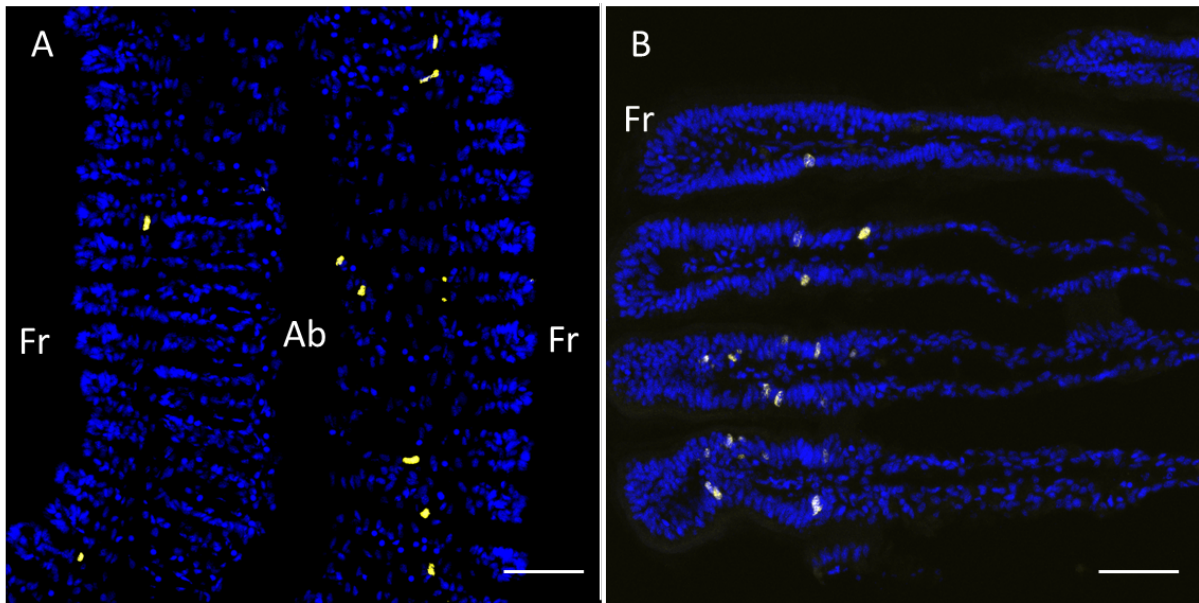
439

440

441 **Figure 2:** Gill filaments of *Bathymodiolus azoricus* labeled with EdU ($3\text{mg}\cdot\text{L}^{-1}$ EdU, 2 hours). Hoechst (blue)
 442 labels the nuclei and symbiotic bacteria, and EdU (yellow) labels the nuclei of the cells which have undergone cell
 443 division during EdU incubation. **A:** Frontal zone of the filament with the frontal ciliated zone (Cz), the ciliated
 444 inter-filament junction (Cj) and the bacteriocytes zone (Bz). Note that most EdU labeled cells are located in the
 445 Cz and Cj, and in the most frontal zone of bacteriocytes, close to Cj, while the more distant area of Bz is devoid
 446 of labeling. **B:** Detail of a ciliated zone, showing nuclei at various stages of cell division. Scale bars: $50\ \mu\text{m}$.

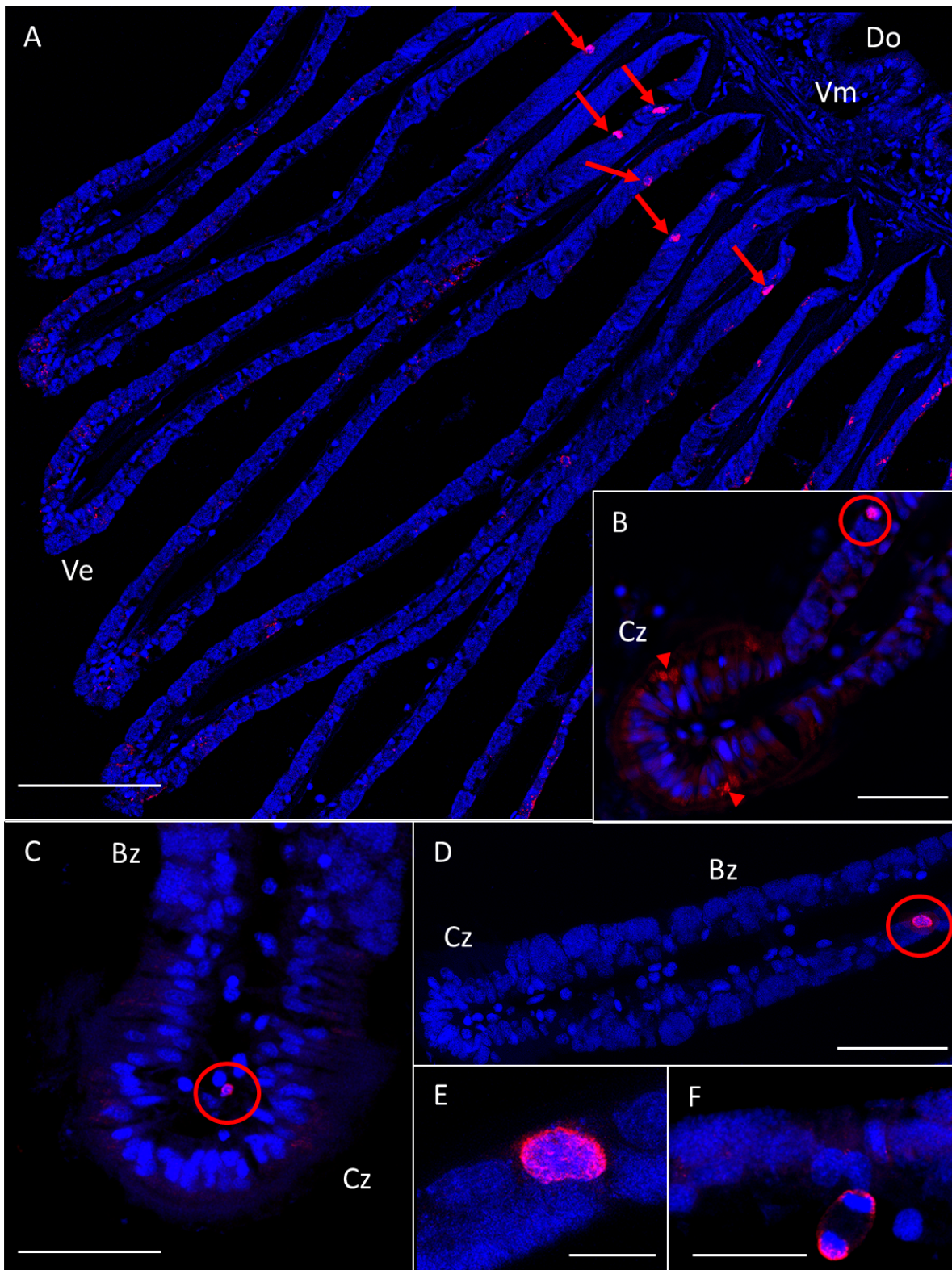
447

448
449



450
451
452
453
454
455

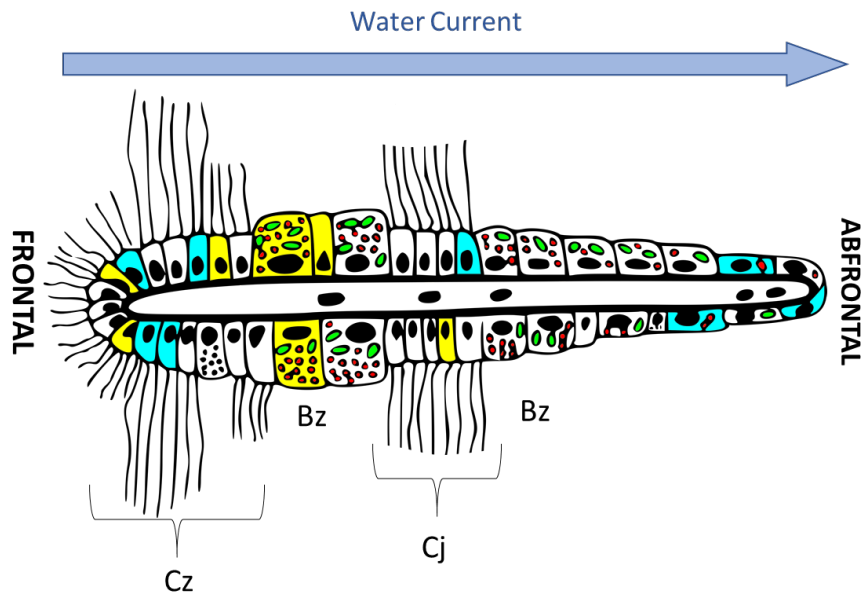
Figure 3: Cell proliferation patterns in isolated gills of *Mytilus edulis*. Hoechst (blue) labels nuclei, and EdU (yellow) labels nuclei of cells undergoing division; frontal (Fr) and abfrontal (Ab) zones are indicated. **A:** 3 mg.L⁻¹ EdU for 5 hours incubation. **B:** 100 mg.L⁻¹ EdU for 5 hours incubation. Scale bars:50 μm.



457

458 **Figure 4:** Gill filaments of *Bathymodiolus azoricus* labeled with DAPI (blue) and anti-PH3 antibody (pink). **A:**
 459 Ventral (Ve) to dorsal (Do) parasagittal section of the gill showing several PH3-labeled cells (red arrows) on the
 460 dorsal side near the visceral mass (Vm). Scale bar : 100 μ m. **B:** Detail displaying an unambiguous label
 461 overlapping with DAPI-labeled nuclei (circled), versus labels that do not overlap with nuclei in the ciliated zone

462 (Cz; arrowheads), likely representing non-specific labeling. Scale bar : 50µm. **C:** The red circle marks a hemocyte
463 undergoing mitosis. Scale bar : 50µm. **D:** A dividing cell in the bacteriocyte zone (Bz, circle). Scale bar : 50µm.
464 **E:** Magnification of figure D, showing the dividing nucleus. Scale bar : 10µm. **F:** Crescent-like PH3 labeling
465 located around the nuclei of two daughter cells shortly after anaphase. Scale bar : 20µm.
466



468

469 **Figure 5:** Schematic cross section of a gill filament of *Bathymodiolus azoricus* summarizing observations from
 470 this study. Areas of cell multiplication are in yellow, mostly located in the frontal ciliated zone (Cz) and in the
 471 bacteriocytes zone (Bz) located near the frontal zone. Areas of cell apoptosis are in cyan, also abundant in the
 472 frontal ciliated zone, but also in the abfrontal zone (Ab) where bacteriocytes tend to be thinner and almost devoid
 473 of bacterial symbionts (after Piquet et al. 2019). Other abbreviations; ciliated junction (Cj).